Proceedings of 6th ICCHMT
May 18–21, 2009, Guangzhou, CHINA
270

FREE-CONVECTION FLOW THROUGH A TWO-DIMENSIONAL BOX WITH OPENINGS ON OPPOSITE WALLS

B P Huynh
Faculty of Engineering & IT, University of Technology, Sydney
PO Box 123, Broadway, NSW 2007, Australia
Fax: +61-2-9514 2655 Email: Phuoc.Huynh@uts.edu.au

ABSTRACT

Free-convection flow through a two-dimensional rectangular box having openings at opposite corners on the vertical walls is investigated numerically, using a commercial Computational Fluid Dynamics (CFD) software package. Convection is induced when the box's ceiling or its floor is imposed with a temperature that is different to that of the ambient fluid, while all other walls are insulated. The fluid here is air near standard conditions, with a molecular Prandtl number of 0.707. Computation is performed for a range of Rayleigh-number values, up to about 2.7×10^9. Chien's turbulence model of low-Reynolds-number K-ε is used. When convection is induced by a cold roof or a hot floor, higher flow rate and heat transfer occur. However the resultant flow and temperature variation are more confined to the wall regions, while the rest of the box is relatively much less affected. All this is in contrast to when convection is due to a hot roof or a cold floor.

NOMENCLATURE

C_μ turbulence-model constant
K turbulent kinetic energy
m fluid's mass flow rate through the box
u_τ friction velocity = $(\tau_w/\rho)^{1/2}$
V velocity magnitude
y^+ non-dimensional distance from closest wall = $\delta/(\nu/u_\tau)$
δ distance from closest wall
α (molecular) thermal diffusivity = $k / (\rho\, c_p)$
β thermal expansion coefficient
ε turbulent kinetic energy's dissipation rate
κ Karman constant
ν (molecular) kinematic viscosity
τ_w wall shear stress

Subscripts

a: ambient fluid
t: turbulent

INTRODUCTION

Room ventilation has always been an important aspect of living, especially in modern living, and this type of flow has attracted much attention [1-11]. Among the methods used to investigate ventilation and related flows, Computational Fluid Dynamics (CFD) has been seen to yield quite adequate results, thus providing a viable alternative or a supplement to experiments [1-3, 7-10]. In these flows natural or free convection is often an important mechanism in transporting heat and mass [1-7, 11]. This paper thus considers free-convection flow through a two-dimensional rectangular box which has two openings on its opposite vertical walls. The flow is induced by either the box's roof or its floor that is set at a temperature different to that of the moving fluid, which is air here. This flow is much related to ventilation, in which the box can be considered as a scaled model of a room. The two-dimensional configuration adopted in this work can be considered as a good approximation to situations wherein the ratio of the room width (the dimension in the ignored 3rd direction) over the openings' height is more than about 20 [10, 12].

MODELLING AND COMPUTATION

The flow model is depicted in Figure 1. A two-dimensional rectangular box of width D = 0.3 m and height D + h = 0.33 m is considered. Two openings of height h = 0.1D = 0.03 m are located on opposite corners of the opposite vertical walls. A Cartesian co-ordinate system is used with the origin positioned

at the bottom left corner of the computational flow domain, x being the horizontal co-ordinate, and y the vertical co-ordinate.

All fluid properties are assumed to be constant and corresponding to those of air at 300 K and standard pressure at sea level (101.3 kPa); but Boussinesq approximation is also assumed for the buoyancy force arising from density variation as a result of temperature change. The following values of molecular properties are used: $\rho = 1.161$ kg/m^3; $\mu = 1.846\times10^{-5}$ N-s/m^2; $\nu = 1.589\times10^{-5}$ m^2/s; $k = 0.0263$ W/m-K; $c_p = 1007$ J/kg-K; $\alpha = 2.25\times10^{-5}$ m^2/s; $Pr = \nu/\alpha = 0.707$; $\beta = 1/T_a = 1/300$ K^{-1}.

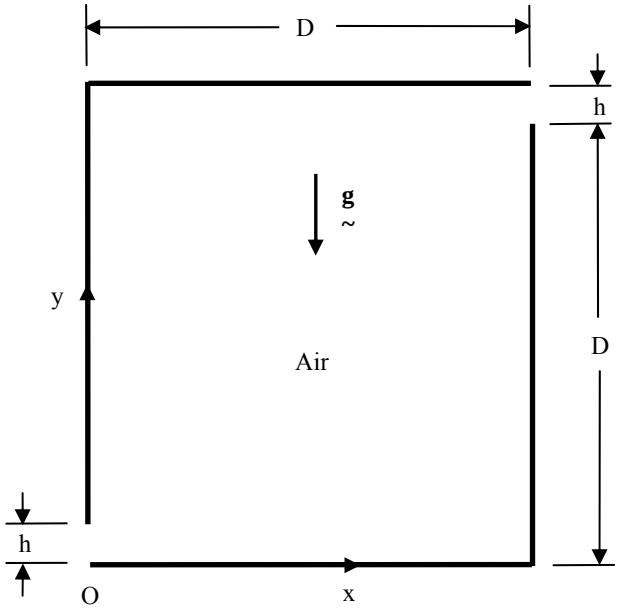

Figure 1. Geometry of the computational domain; D = 0.3 m, h = 0.1 D. A Cartesian co-ordinate system has been used with origin at O, horizontal distance x, and vertical distance y.

With these values, the Rayleigh number Ra, which is a key parameter in free convection, and based on D, is $Ra = 2.47\times10^6\Delta T$, wherein ΔT is the difference between either the floor or roof temperature and the ambient temperature (300 K).

Since turbulence is expected at $Ra > 10^6$ for free convection in similar configurations [13-14], all cases considered in this work are taken to be in the turbulent regime. Turbulent Prandtl number is taken to be constant at $Pr_t = 0.9$, following a suggestion by, for example, Burmeister [15].

A Reynolds-Averaged Navier-Stokes (RANS) formulation is used, wherein turbulence affects the mean flow through a turbulent viscosity μ_t; turbulent stresses are assumed to be proportional to the mean rates of strain via μ_t. The low-Reynolds-number K-ε turbulence model of Chien [16] is adopted. Thus, governing equations are those of Reynolds-averaged conservation of mass and momentum, and balance of energy, plus the two transport equations for K and ε of the Chien's model.

Referring to Figure 1, boundary conditions for the mean variables (velocity components, pressure and temperature) are as follows

- The two openings represent the ambient conditions; the fluid has constant ambient pressure and temperature, namely p = 0 (gauge, without the hydrostatic component), $T = T_a = 300$ K (27 ºC). However, the thermal condition here applies only on those sections of the boundary where there is inflow; if the computation reveals outflow on any sections, the constant temperature condition there will be ignored; instead, temperature will be computed. Similarly, the constant pressure condition applies only on those sections of the boundary where there is outflow; if the computation reveals inflow on any sections, the constant pressure condition there will be ignored, and pressure will be computed instead
- Isothermal wall conditions are prescribed on either the floor or the roof of the box: zero velocity u = v = 0, plus either $T = T_{floor}$ (isothermal floor) or $T = T_{roof}$ (isothermal roof)
- All other walls (except the isothermal floor or roof as described above) are adiabatic (insulated): zero velocity u = v = 0; $\partial T/\partial y = 0$

As regards the turbulence-model variables K and ε, they are prescribed as follows

- On the two vertical walls, floor and roof: default solid-surface condition of the software package (see below) is adopted; this entails K = 0 and ε = 0, following Chien [16]
- At the two openings which represent the ambient conditions, K and ε are assumed to be constant. The manner of prescribing their values is discussed next below. However, these conditions apply only on those sections of the boundary where there is inflow; if the computation reveals outflow on any sections, the conditions of prescribing values for K and ε there will be ignored; instead, K and ε will be computed

It is found that turbulence level prescribed at the openings as boundary conditions has very small effects on the results. Thus, for example, the following 3 cases have been computed and compared, all with T_{roof} = ***330 K***. In case 1, an arbitrary value of $K = 1\times10^{-4}$ m^2/s^2 and $\varepsilon = 5\times10^{-5}$ m^2/s^3 are prescribed at the openings. The following results are obtained: Net mass flow rate through the openings $m = 8.2044\times10^{-4}$ kg/s-m, heat transfer rate through the lower opening $Q_{open\text{-}low}$ = 247.86 W/m, heat transfer rate through the roof Q_{roof} = 14.000 W/m. The average flow velocity through the openings is thus U = 0.02355 m/s. In case 2, a moderate level of turbulence intensity of 5 % is assumed, using U computed from case 1 above, so that $K = (3/2)\times(0.05U)^2 = 2.08\times10^{-6}$ m^2/s^2. ε is assumed to be related to K via the common relationship $\varepsilon = (C_\mu)^{3/4}K^{3/2}/(\kappa h) = 4.11\times10^{-8}$ m^2/s^3, wherein C_μ = 0.09 being a turbulence-model constant, and κ = 0.4 being the Karman constant. With these new K and ε values imposed on the openings, the computational results are nearly the same as those of case 1 above. More specifically, case 2 results in $m = 8.2060\times10^{-4}$ kg/s-m, $Q_{open\text{-}low}$ = 247.90 W/m, Q_{roof} = 14.022 W/m. Relative differences between these and the corresponding case 1's values are 0.02 %, 0.02 %, and 0.16 % respectively. In case 3, K = 0 and ε = 0 are imposed at the openings. This results in $m = 8.2231\times10^{-4}$ kg/s-m, $Q_{open\text{-}low}$ = 248.42 W/m, Q_{roof} = 14.026 W/m. Relative differences between these and the corresponding case 2's values are thus 0.21 %, 0.21 %, and 0.03 % respectively.

From considerations similar to those above, a boundary value pair of $K = 2.08\times10^{-6}$ m^2/s^2 and $\varepsilon = 4.11\times10^{-8}$ m^2/s^3 has been used at the two openings.

The commercial software package CFD-ACE from the ESI Group is used for the computation. The package is quite well known, and its validation is thus assumed to have been adequate. In addition, some further tests had added positively to its validity; see, for example, Huynh [17]. The numerical scheme is the Finite Volume method, and the coupled system of governing equations is solved iteratively for the two mean velocity components, mean temperature and pressure, plus K and ε.

A convergence criterion of reduction of residuals in the solved variables by 3 orders of magnitude is adopted. This is deemed adequate; a comparison of the solutions with residual reduction of 3 orders of magnitude and those with residual reduction of 4 orders of magnitude shows very small difference. Thus, for example, with the case of T_{floor} = 280 K, the relative difference in the net mass in-flow through the upper opening is only 3.4×10^{-4} (7.2706×10^{-4} kg/s-m versus 7.2731×10^{-4} kg/s-m). All computation is done with double precision (64 bits).

Grid convergence tests have also been performed to ascertain the adequacy of the grid patterns used. Thus, for example, with the case of T_{floor} = 280 K, as the number of grid points on the pair of a vertical solid wall and opening is increased from 125-25 (125 on wall, 25 on opening) to 150-30, change in the net mass in-flow through the upper opening is only 0.55%. Similar variations are also seen with other cases. From such tests, patterns with 150 grid points on each of the solid walls and 30 grid points on each of the openings are deemed adequate and used.

Also, post-solution checks of y^+ values of grid points closest to the walls show y^+ being well below 1, thus confirming that the grid patterns used are sufficiently fine for the Chien's turbulence model.

RESULTS AND DISCUSSION

Fig. 2 shows the net mass flow rate through the box with respect to the difference between roof temperature and ambient temperature, $\Delta T_{roof} = T_{roof} - T_a$. Note that very good symmetry exists, as it should be, between cases of roof temperature difference ΔT_{roof} and corresponding floor temperature difference $\Delta T_{floor} = T_{floor} - T_a = -\Delta T_{roof}$. Thus, for example, nearly identical flow pattern, temperature distribution, mass flow rate, pressure contours, etc., exist for the pair of ΔT_{roof} = 20 K and ΔT_{floor} = – 20 K, or for the pair ΔT_{roof} = – 30 K and ΔT_{floor} = 30 K.

Fig. 2 shows that a roof cooled by ΔT below the ambient temperature causes much more air flow through the box than if it is heated by the same ΔT above the ambient. Also, mass flow rate m increases rapidly with lower T_{roof} when the roof is cooler than the ambient air, in contrast to when it is hotter; then, as T_{roof} increases above T_a, m also increases but soon reaches saturation. Thus, very small increases in m occur with higher ΔT_{roof} when this is above about 10 K.

Fig. 2 indicates that, for example, if a large amount of cooled air is desired, then a cooled roof is much more effective than a cooled floor (whose flow is equivalent to a heated roof's); or, if a large amount of heated air is desired, then a heated floor (whose flow is equivalent to a cooled roof's) is much more effective than a heated roof.

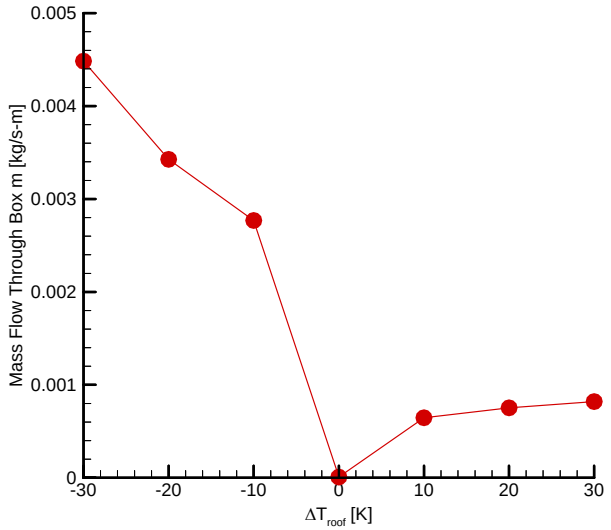

Figure 2. Mass flow rate through the box versus difference between roof temperature and ambient temperature.

Figure 3 shows variation of mean velocities V_{mean} with respect to ΔT_{roof}, for the box's 3 zones and for the whole box itself. The zones are defined as follows: zone 1 is the middle region between the openings (height level between h to D above the floor), zone 2 the horizontal region containing the upper opening next to the roof (height level between D to D + h above the floor), zone 3 the horizontal region containing the lower opening next to the floor (height level between 0 to h above the floor). The curves' pattern in general follows that of air mass shown in Figure 2. Also, as expected, zone 2, which is closest to the roof, is the most affected by ΔT_{roof}, and thus has highest mean velocity. The large difference between mean velocity of zone 2 (the roof region) and that of other zones also indicates that most of the flow occurs close to the non-isothermal wall (in this case the roof), be it cooled or heated. While this is also expected, the scale of the difference could be of interest.

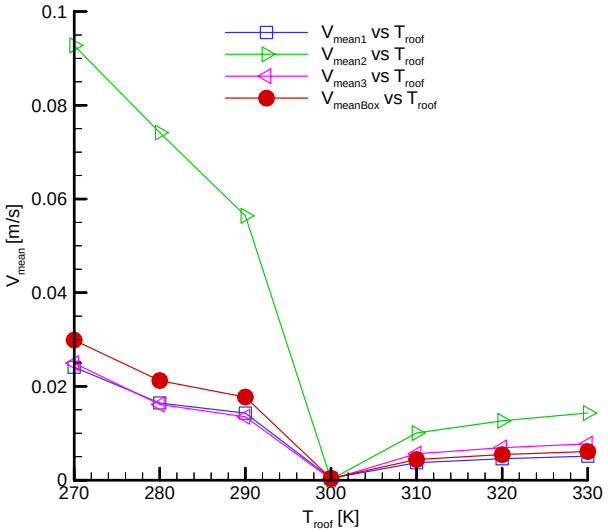

Figure 3. Mean velocity in the 3 zones and for the whole box versus roof temperature. The zones are described in the text.

Heat transfer through the roof is shown in Figure 4 as a plot of Q_{roof} versus ΔT_{roof}. While Q_{roof} increasing uniformly with higher ΔT_{roof} is expected, the curve's slope can be seen to decrease moderately and is lowest when ΔT_{roof} is about zero, before increasing again, also moderately. This indicates that Q_{roof} changes slightly faster for larger $|\Delta T_{roof}|$, a result that would agree with expectation; for, larger $|\Delta T_{roof}|$ also increases flow velocity as per Figure 3, and higher velocity transports more heat.

Furthermore, Figure 4 also shows that a cooled roof transfers more net heat than a heated one, for the same $|\Delta T_{roof}|$. Thus, for example, if large amounts of heat are to be removed from the air flowing through the box, a cooled roof is more effective than a cooled floor. Similarly, if large amounts of heat are to be added, then a heated floor is more effective than a heated roof. This is also in agreement with expectation. For, taking the case of removing heat from the box' air via a cooled roof, since cooled fluid tends to sink to the box' floor while hotter fluid stays close to the roof, a larger temperature difference would exist between the hot fluid and the cooled roof. The result is a larger heat transfer rate. Temperature gradients adjacent to a cooled roof can be seen to be mostly stiffer than those adjacent to a cooled floor in Figures 6 and 7 below.

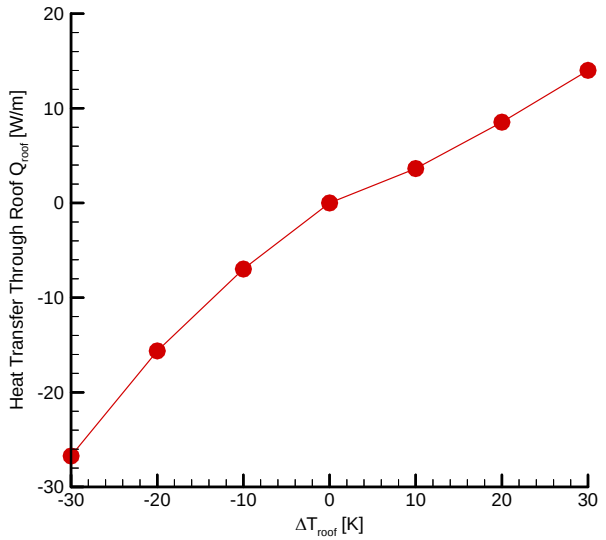

Figure 4. Heat transfer rate through the roof versus difference between roof temperature and ambient temperature.

Mean temperature in the 3 zones and for the whole box are shown in terms of roof temperature in Figure 5. The curves' pattern of uniform increase with T_{roof} is in general similar to that of Q_{roof} shown in Figure 4. Also, as expected, zone 2, which is adjacent to the roof, shows largest change in its mean temperature. The slope in this zone, however, varies in an opposite way to that of Q_{roof}. Thus, T_{mean} varies more rapidly near zero $|\Delta T_{roof}|$ (or $T_{roof} = T_a = 300$ K), in contrast to Q_{roof}. This can be explained as follows. With small $|\Delta T_{roof}|$, the region that is affected by any change in the roof temperature is also small, in other words, well confined to zone 2. The result is that this zone's temperature is strongly affected by T_{roof}. On the other hand, at large $|\Delta T_{roof}|$, the affected region would spread out into other zones. The consequence is that temperature in zone 2 (adjacent to the roof) would thus be less sensitive to changes in T_{roof}.

Figure 6 shows the flow pattern, velocity and temperature distributions for a representative case of cooled floor ($T_{floor} = 280$ K, or $\Delta T_{floor} = T_{floor} - T_a = -20$ K). These pattern and distributions should be similar to the case of heated roof with corresponding $\Delta T_{roof} = T_{roof} - T_a = 20$ K. On the other hand, Figure 7 shows a representative case of cooled roof ($T_{roof} = 280$ K, or $\Delta T_{roof} = -20$ K) (or, equivalently, a heated floor with $\Delta T_{floor} = 20$ K). These figures show that with a cooled floor (or a heated roof), the flow affects nearly the whole box, whereas with a cooled roof (or a heated floor) the flow is confined mainly along the affected horizontal wall and the vertical wall that has the exit opening on it. Also, as mentioned above, the temperature gradient is somewhat stiffer on a cooled roof than on a cooled floor. This results in a larger heat transfer rate on a cooled roof than on a cooled floor, as also mentioned above.

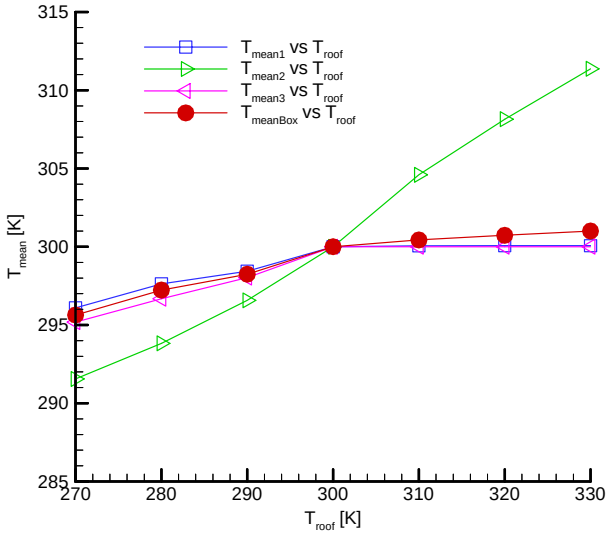

Figure 5. Mean temperature in the 3 zones and for the whole box, versus roof temperature.

CONCLUSIONS

Free-convection flow has been investigated numerically for a two-dimensional rectangular box with openings on opposite corners on its vertical walls. The box has one horizontal wall (floor or roof) being isothermal, while all other three walls are adiabatic. A cooled roof (or correspondingly a heated floor) induces more flow through the box, as well as higher heat transfer rate through the non-isothermal wall, than a cooled floor (or a heated roof). However, a cooled floor induces flow that affects nearly the whole box, in contrast to a cooled roof; in this case, flow is more confined to the affected horizontal wall (cooled roof) and the vertical wall with the exit opening on it. In other words, cooled roofs (or heated floors) produce stronger but more confined flow, than cooled floors (or heated roofs).

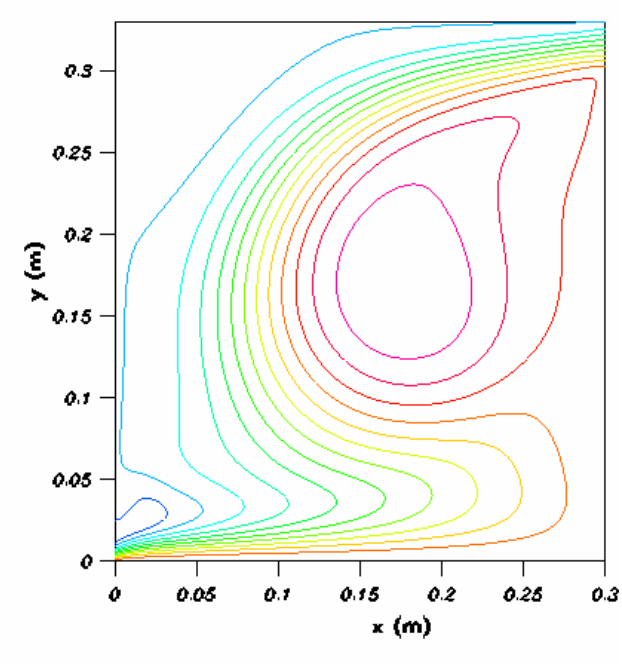

(6a)

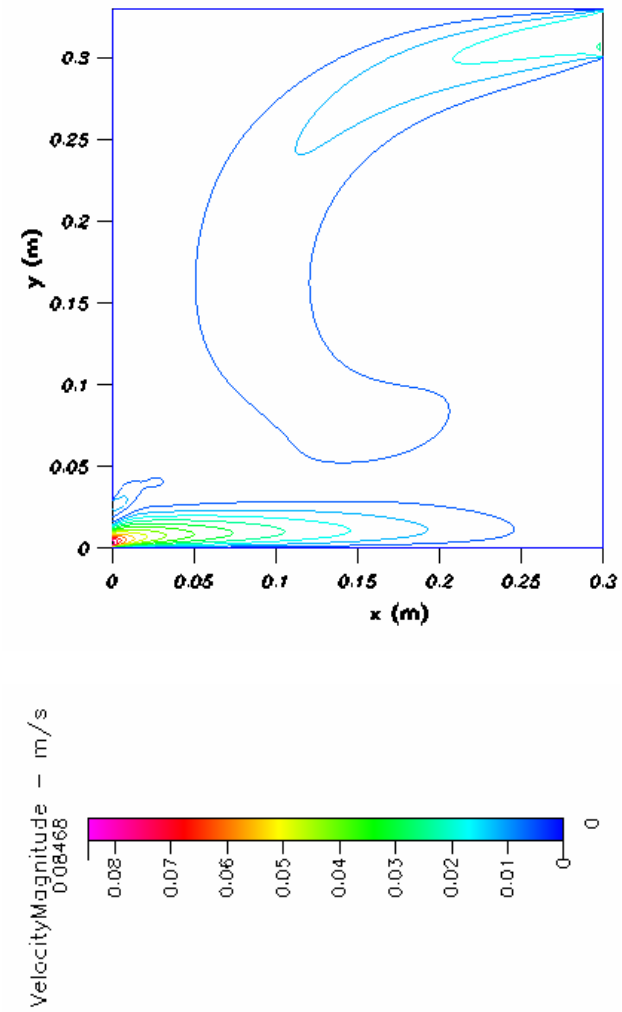

(6b)

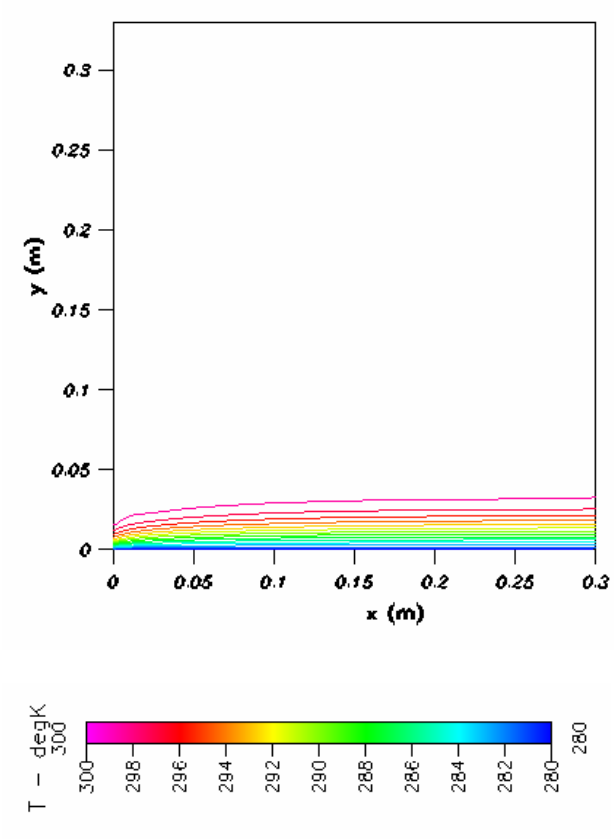

(6c)

Figure 6. Streamlines (6a), contours of velocity magnitudes (6b), and temperature distribution (6c), of case of T_{floor} = 280 K (ΔT_{floor} = −20 K).

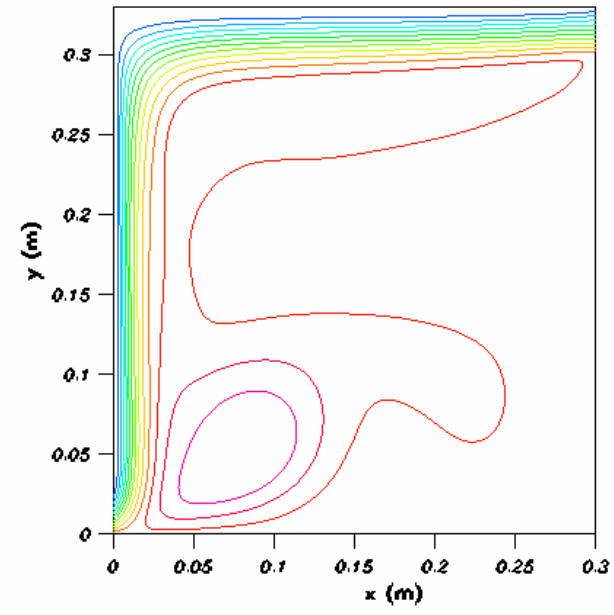

(7a)

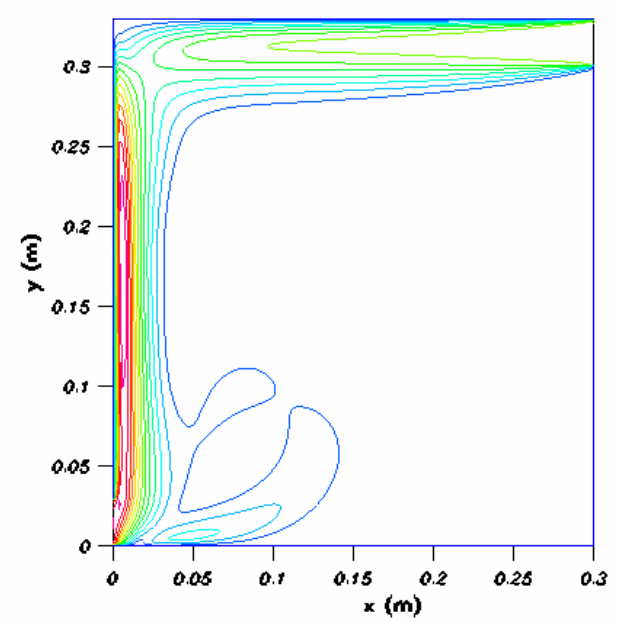

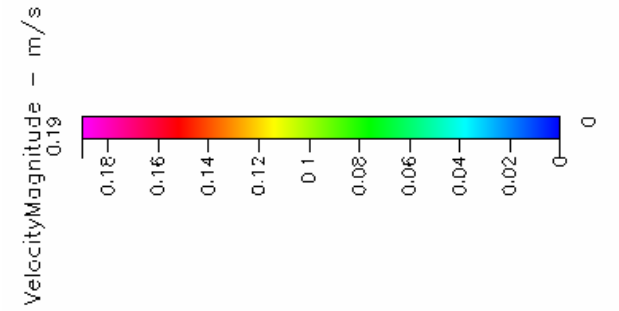

(7b)

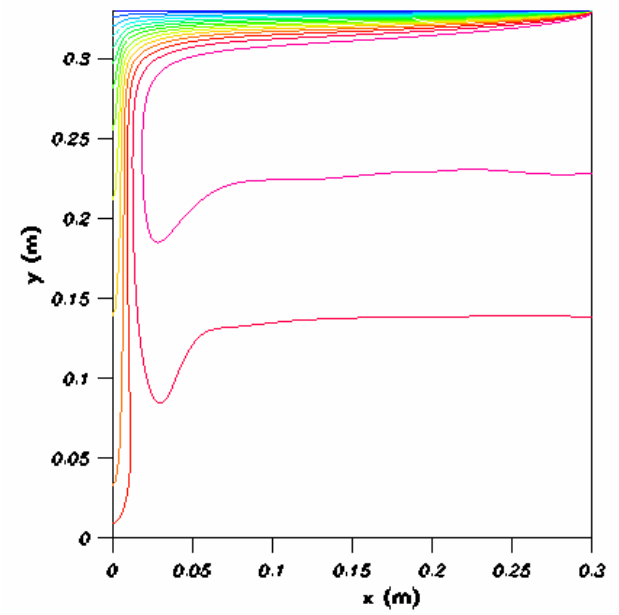

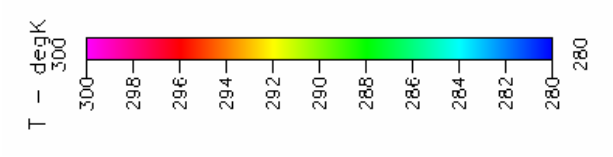

(7c)

Figure 7. Streamlines (7a), contours of velocity magnitudes (7b), and temperature distribution (7c), of case of $T_{roof} = 280$ K ($\Delta T_{roof} = -20$ K).

REFERENCES

1. Awbi, H.B., 1989, Application of Computational Fluid Dynamics in Room Ventilation, *Building and Environment*, **24**, pp. 73-84.
2. Davidson, L., 1989, Ventilation by Displacement in a Three-Dimensional Room – A Numerical Study, *Building and Environment*, **24**, pp. 363-372.
3. Chen, Q., 1995, Comparison of Different k-ε Models for Indoor Air Flow Computations, *Numerical Heat Transfer, Part B*, **28**, pp. 353-369.
4. Xue, H. and Shu, C., 1999, Mixing Characteristics in a Ventilated Room With Non-isothermal Ceiling Air Supply, *Building and Environment*, **34**, pp. 245-251.
5. Rodrigues, A.M. et al., 2000, Modelling Natural Convection in a Heated Vertical Channel for Room Ventilation, *Building and Environment*, **35**, pp. 455-469.
6. Park, H.-J. and Holland, D., 2001, The Effect of Location of a Convective Heat Source on Displacement Ventilation: CFD Study, *Building and Environment*, **36**, pp. 883-889.
7. Lu, W.Z. et al., 2002, Numerical Investigation of Convection Heat Transfer in a Heated Room, *Numerical Heat Transfer, Part A*, **42**, pp. 233-251.
8. Posner, J.D. et al., 2003, Measurement and Prediction of Indoor Air Flow in a Model Room, *Energy and Buildings*, **35**, pp. 515-526.
9. Tian, Z.F. et al., 2006, On the Numerical Study of Contaminant Particle Concentration in Indoor Airflow, *Building and Environment*, **41**, pp. 1504-1514.
10. Wang, X. et al., 2007, Numerical Study of Air Movement in a Slot-Ventilated Enclosure, *ASHRAE Transactions*, **113**, pp. 400-405.

11. Tanny, J. et al., 2008, Airflow and Heat Flux Through the Vertical Opening of Buoyancy-Induced Naturally ventilated Enclosures, *Energy and Buildings*, **40**, pp. 637-646.
12. Forthmann, E., 1934, Turbulent Jet Expansion, *Technical Memorandum 789*, NACA
13. Elder, J.W., 1965, Turbulent Free Convection in a Vertical Slot, *Journal of Fluid Mechanics*, **23**, pp. 99-111.
14. Markatos, N.C. and Pericleous, A.K., 1984, Laminar and Turbulent Natural Convection in an Enclosed Cavity, *International Journal of Heat & Mass Transfer*, **27**, pp. 755-772.
15. Burmeister, L.C., 1993, *Convective Heat Transfer,* 2nd Ed., Wiley, New York.
16. Chien, K.-Y., 1982, Predictions of Channel and Boundary-Layer Flows with a Low-Reynolds-Number Turbulence Model, *AIAA Journal*, **20**, pp. 33-38.
17. Huynh, B.P., 2006, Free Convection Cooling of a Horizontal Cylinder Positioned Above a Plane, *Proceedings of the 13th International Heat Transfer Conference*, Sydney, Australia, 13-18 August, Paper NCV-46.

6TH INTERNATIONAL CONFERENCE ON COMPUTATIONAL HEAT AND MASS TRANSFER

Guangzhou, China, May 18-21, 2009